Simulation of an Auto-Tuning Bicycle Suspension Fork with Quick Releasing Valves

Y. C. Mao, and G. S. Chen

Abstract—Bicycle configuration is not as large as those of motorcycles or automobiles, while it indeed composes a complicated dynamic system. People's requirements on comfortability, controllability and safety grow higher as the research and development technologies improve. The shock absorber affects the vehicle suspension performances enormously. The absorber takes the vibration energy and releases it at a suitable time, keeping the wheel under a proper contact condition with road surface, maintaining the vehicle chassis stability. Suspension design for mountain bicycles is more difficult than that of city bikes since it encounters dynamic variations on road and loading conditions. Riders need a stiff damper as they exert to tread on the pedals when climbing, while a soft damper when they descend downhill. Various switchable shock absorbers are proposed in markets, however riders have to manually switch them among soft, hard and lock positions. This study proposes a novel design of the bicycle shock absorber, which provides automatic smooth tuning of the damping coefficient, from a predetermined lower bound to theoretically unlimited. An automatic quick releasing valve is involved in this design so that it can release the peak pressure when the suspension fork runs into a square-wave type obstacle and prevent the chassis from damage, avoiding the rider skeleton from injury. This design achieves the automatic tuning process by innovative plunger valve and fluidic passage arrangements without any electronic devices. Theoretical modelling of the damper and spring are established in this study. Design parameters of the valves and fluidic passages are determined. Relations between design parameters and shock absorber performances are discussed in this paper. The analytical results give directions to the shock absorber manufacture.

Keywords—Modelling, Simulation, Bicycle, Shock Absorber, Damping, Releasing Valve.

I. INTRODUCTION

A. Background

Compared with automobiles and motorcycles, bicycles construct a smaller structure yet complicated system with more than 2000 components. These components can be divided into several subsystems, including the frame, transmission, wheel, steering, brake and accessory subsystems. The front suspension fork and rear shock absorber, such as the apparatuses shown in Fig. 1, are

Y.C. Mao is with the Department of Mechanical Design Engineering, National Formosa University, Yun-lin County 632, Taiwan R.O.C. (+886-5-6315348; Fax: 886-5-6363010; email: yjmau63@gmail.com)

G.S. Chen is the Research and Development Department Manager, SPINNER Industry Co., Ltd., No.34, Jiahou Rd., Waipu Township, Taichung County 438, Taiwan R.O.C.

important parts in the frame system since they significantly affect the riding comfort and safety.

Fig. 1 The SPINNER® Cargo Air RLC Suspension Fork

A feasible suspension system holds the following capabilities:

1) Vibration isolation. The suspension system has to isolate disturbances from the road surface, acceleration and load-transferring effect of the vehicle chassis, thus it can provide a stable operation for drivers.

2) Energy dissipation. The suspension system stabilizes the vehicle chassis in a short period of time. The system conditions the vehicle body controllability and rider safety by keeping the contact forces between wheels and road surface within a feasible range.

3) Coordination among shock absorbers. The individual shock absorber collaborates with others to adjust the road-wheel contact forces according to the road surface, chassis and loading conditions [1].

B. Technology Classification

Vehicle suspension systems can be categorized into three types, namely the passive, semi-active and active suspension systems, as shown in Fig. 2 [1].

The passive suspension system, as illustrated in Fig. 2a, composes a constant spring and damper. The spring is utilized to support the vehicle body and store the rebound energy. The damper functions as a dissipater to eliminate the transient energy [2]. The dynamic property of this type is fixed regardless of the road surface and load conditions since it occupies a spring and damper of constant values. The factory setting for this type of suspension system is a critical issue and can only meet a restricted operation condition range.

(a) Passive suspension   (b) Semiactive suspension   (c) Active suspension
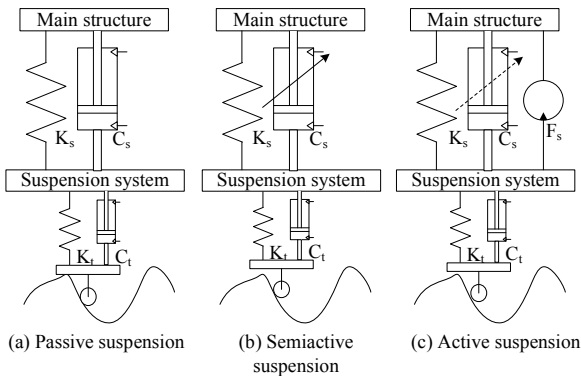
Fig. 2 Schemes of vehicle suspension systems

Related works proposed the active suspension configurations to overcome the above-mentioned defects, as shown in Fig. 2c. Sensors and actuators with properly developed control algorithms can optimize the vehicle dynamics, restraining wheel bounds and chassis tilts. The Bose Suspension System draws the support from a linear electromagnetic motor to achieve the vehicle stability and comfort [3]. Active suspension systems, however, usually comprise of complicated costly peripherals, restricting their practical applications. The working frequency is limited to the input power. It is feasible to be equipped with an automobile system, applying on the low frequency chassis attitude control. The active suspension system is not suitable for a low- or human-powered mobile system, such as the motorcycle or bicycle [4].

Compared with the above two configurations, Fig. 2b represents a semi-active suspension system which attracts considerable research efforts, since it is capable of tuning the damping coefficient adaptively according to the driving condition [1]. This type of configuration is incapable of balancing the chassis tilts however it can adjust its damping coefficient with limited power consumption [4-5]. The damping force is adjusted in a predetermined range according to different piston velocity, as shown in Fig. 3.
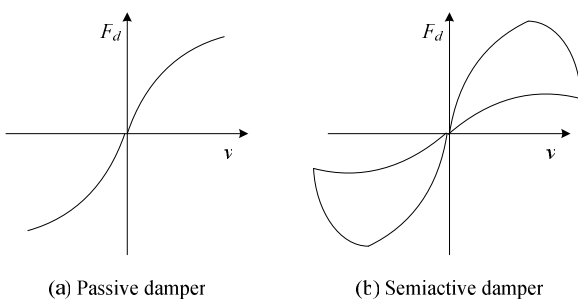

(a) Passive damper   (b) Semiactive damper

Fig. 3 Curves of velocities-forces for passive and semi-active dampers [5]

The fluidic circuit inside the shock damper has to involve a sensory mechanism to determine the system position, velocity or acceleration, thus the semi-active system can adjust its parameters by certain means. There are at least three types of means that can alter the damping coefficient:

1) Structural friction force. This type employs an electromagnetic motor or other mechanical energy output device to control the normal force between contact components, altering the friction force therefore varying the vibration energy dissipation.

2) Fluid viscosity in the damper. These dampers fill at least part of the cylinder chambers with electro- or magneto-rheological fluid. The fluid viscosity is changed as the electric or magnetic field varies, altering the resistant force of the damper.

3) Orifice area control. The orifice area controls the flow rate among passages and chambers, changing the damping force of the shock absorber.

Due to the limited space, power supply deficiency and weight requirement, a great part of damper designs of the bicycle shock absorbers focuses on the orifice area control.

C. Related Works

Considering the fluid dynamics, Mollica and Youcef-Toumi proposed a physical model for a high pressure monotube shock absorber to analyze the nonlinear dynamic behavior of these dampers [6]. Results explained that the hysteresis frequency dependency is produced by the interaction at higher frequencies that results in added phase loss due to the capacitive elements. Goncalves evaluated the dynamic response of different semi-active control policies over a magneto-rheological damper as tested on a single suspension quarter-car system [7]. Bathe et al. presented advances in capabilities for the analysis of fluid flows with structural interactions [8]. An arbitrary Lagrangian-Eulerian formulation is used to solve for the fluid response with structural interface and free surface conditions. Beghi et al. involved a grey-box modeling technique to describe the complex behavior of motorcycle shock absorbers, exhibiting a significant improvement in the force prediction capability over traditional linear models [9]. Yang et al. designed a new shock absorber with Coulomb–fluid damping through coupling oil, wire gauze, rubber and spring for reinforcement of electronic-information equipment in vibration and impact [10]. The nonlinear dynamic model for attenuating vibration mode is derived from coupling physical mechanism of fluid and Coulomb friction.

In the field of vehicle system dynamics, Wang and Hull proposed a model for determining rider induced energy losses in bicycle suspension systems [11]. Ignoring the terrain irregularities, the power dissipated by the stiffness and dissipative characteristics of the suspension elements was calculated. Pracny et al. performed a dynamic full vehicle simulation using a thermo-mechanically coupled hybrid neural network shock absorber model [12]. In this shock absorber model, the spline approach is combined with a temperature-dependent neural network, simulated on a test rig in ADAMS-Car multi-body simulation software with a displacement-controlled excitation.

As there is currently no infrastructure available to test the shock absorbers' performance, Heritier built a test rig allowing the performance characteristics of the various damper settings

to be explored and vehicle performance to be optimized [13]. Titlestad *et al.* built a test rig, simulating regular impacts of the rear wheel with bumps in a rolling road, measuring physiological variables of oxygen consumption and heart rate, together with speeds and forces at various points in that system.

II. THE PROPOSED DESIGN

A. Design Goal

A significant defect of suspended bicycles is the tendency to dissipate pedaling energy through the spring and shock absorber. As the rider imparts force into the pedals the vertical vector component causes the bicycle to bob on its suspension. This undesirable suspension movement dissipates a significant percentage of the imparted pedaling energy and can reduce the bicycle's overall motive efficiency.

A widely adopted solution to this problem is to introduce a "lockout" means for riders to manually operate when desired. The term lockout refers to one or more of the following elements in combination: mechanically limiting the amount of suspension travel; increasing the damping response of the shock absorber, most importantly in compression; increasing the force-displacement rate of the suspension; increasing the spring preload of the suspension. Normally the rider would engage the lockout during heavy pedaling as required by hill climbing or acceleration but could disengage it for coasting and downhill operation over bumpy terrain. The most common form of bicycle suspension lockout consists of a valve that limits the flow of oil past the shock absorber's main piston. The limitation of the manually activated suspension lockout is that it requires the constant attention of a rider already busy with numerous other tractive and control functions.

This research proposes an innovative self-tuning damper with quick releasing (QR) valve of a suspension fork for bicycles. The fundamental idea of the self-tuning mechanism is to set up an orifice with a variable sectional area in the fluid passages inside the damper. This damper automatically tunes the damping coefficient by altering the oil flow rate through the passages according to the input force or velocity. The QR valve keeps inactive during normal operations, while it sluices the peak fluid pressure when the damper encounters square-edged bumps, maintaining the damper softness and preventing the rider limbs from sprained under shock waves. It would therefore be advantageous to automatically lock out the suspension system when required, specifically during uphill riding and rapid acceleration when the rider is pedaling hard. This mechanism automatically quickly releases the lockout as well when the suspension system encounters a downhill operation over bumpy terrain.

B. Apparatus Configuration and Operations

Fig. 4 sketches out the overall configuration of the proposed design, comprising of the key components in a damper side of a twin-tube bicycle front fork. The upper fork is slidely connected within the lower fork. The damping stator is fixed at the upper end of the inner tube. The lower end of the inner tube is immobilized with the lower end of the upper fork. The main piston, synchronally moving with the lower fork, impels and draws the oil in the lower chamber. The fluid, passing through the orifices inside the damping stator, flows back and forth between the upper and lower chambers. The separation film keeps the air in the top chamber from mixing with oil in the upper chamber.
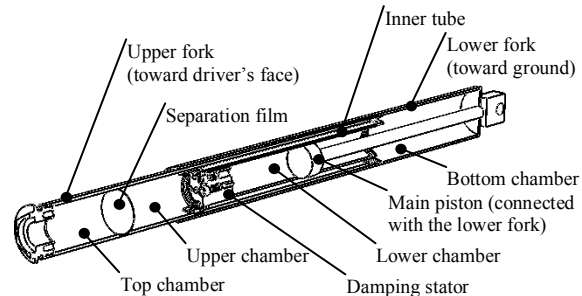

Fig. 4 The overall sectional view of the proposed design

The fluid circuit inside the damping stator is shown in Fig. 5. The spool valve CAD model is shown in Fig. 6, illustrating a double opening design for a wide flowing range. When a certain force drives the main piston toward the upper side of the damper, high-pressure fluid in the lower chamber is impelled into the upper chamber, achieving the pressure-release process.
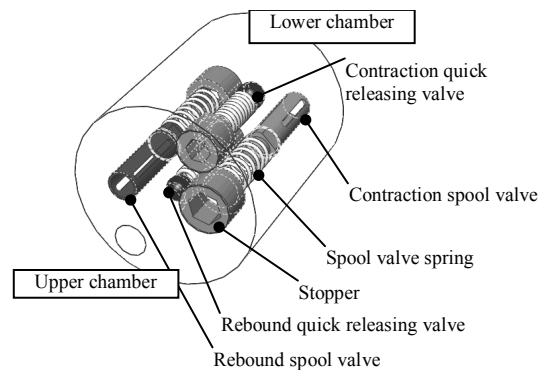

Fig. 5 Fluid circuits inside the damping stator

Take the contraction valves for illustration. The fluid pushes the contraction spool valve against the spring at this moment. The valve keeps closed before the lower chamber pressure rises up to a certain level, functioning as an automatic locking-out capability. The valve together with the tunnel inside the stator open an equivalent orifice and allow the fluid flow through the orifice if the pressure is high enough to balance or surpass the spring force. The damping coefficient is decreased as the equivalent orifice area is increased, achieving an automatic tuning function. If the damper encounters a square-edged bump, the QR valve opens, allowing the peak fluid pressure in the lower chamber to drop down rapidly. The operation manner of the rebound mode is similar to that of the contraction mode. Hence the proposed design automatically adjusts the damping ratio according to a wide road surface
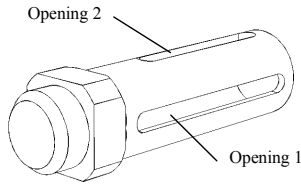
condition.

Fig. 6 CAD model and dimensions of the spool valve

III. MODELLING THE SYSTEM DYNAMICS

The frictional forces between pistons and cylinder walls are neglected in this study. Damping coefficient due to the friction is modeled but set to be zero in this study.

A. System Overview

The physical and mathematical parameters are defined in Fig. 7. Initial volume of the top, upper, lower and bottom chambers are V_{t0}, V_{u0}, V_{l0} and V_{b0}, respectively.
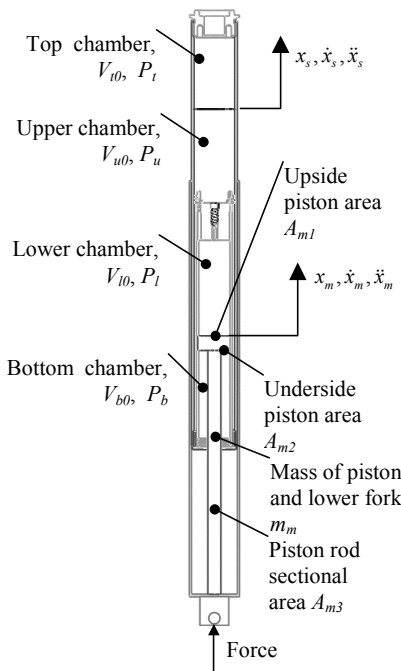

Fig. 7 Mathematical model of the entire damper

B. The Driving Force

The force F_m is modeled as a sinusoid wave with the amplitude of F_0:

$$F_m = F_0 Sin(wt + \phi)$$

where w is a constant angular velocity, ϕ denotes the initial angular position of the driving force. The time-derivative is:

$$\dot{F}_m = F_0 Cos(wt + \phi)$$

C. Main Piston

The resultant force, derived from the driving force and pressures in the bottom and lower chambers, pushes the main piston upward to a certain position x_m.

$$m_m \ddot{x}_m + C_m \dot{x}_m + k_m x_m = F_m - P_l A_{m1} + P_b A_{m2} + P_a A_{m3} - m_m g$$

where C_m is the damping coefficient caused by friction; k_m denotes the main spring in the shock absorber, which is installed in the other side of the fork and not shown in this study; P_a is the atmosphere of 1.0134e5 Pa; g represents the gravity.

D. Damping Stator, Spool Valves and QR Valves

The valve movements induce the damping characteristics of the proposed design, as defined in Fig. 8, which shows the contraction spool and QR valves only. Rebound valves work at the opposite sides in the damping stator, and have similar operating conditions. They slide in the valve tunnels according to the pressures in the lower and upper chambers. For the contraction spool valve:

$$m_{cn} \ddot{x}_{cn} + C_{cn} \dot{x}_{cn} + k_{cn} x_{cn} = P_l A_{cn} - P_u A_{cn} - m_{cn} g$$

while the rebound spool valve's dynamics is:

$$m_{rn} \ddot{x}_{rn} + C_{rn} \dot{x}_{rn} + k_{rn} x_{rn} = -P_l A_{rn} + P_u A_{rn} + m_{rn} g$$

For the contraction QR valve:

$$m_{cb} \ddot{x}_{cb} + C_{cb} \dot{x}_{cb} + k_{cb} x_{cb} = P_l A_{cb} - P_u A_{cb} + m_{cb} g$$

and the rebound QR valve's dynamics can be described as:

$$m_{rb} \ddot{x}_{rb} + C_{rb} \dot{x}_{rb} + k_{rb} x_{rb} = -P_l A_{rb} + P_u A_{rb} - m_{rb} g$$

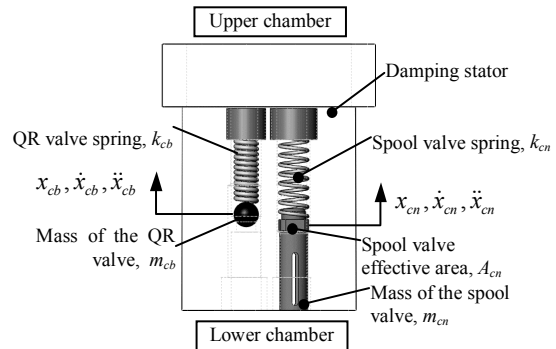where the positive directions of x_{rn} and x_{rb} are toward the ground.

Fig. 8 Model of the contraction valves in the damping stator

E. Separation Film

The separation film is modeled as a piston with an extremely small mass, and frictionless with the cylinder wall. The pressure difference between the upper and top chambers impels its movement:

$$m_s \ddot{x}_s + C_s \dot{x}_s = P_u A_s - P_t A_s - m_s g$$

where m_s represents the mass of the film.

F. Pressure in the Bottom Chamber

The bottom chamber is initially filled with air of 1 atm. The pressure change rate varies with the main piston position and velocity:

$$\dot{P}_b = \gamma \frac{-P_b A_{m2} \dot{x}_m}{V_{b0} + A_{m2} x_m}$$

where γ is the specific heat ratio for air, and is selected as 1.4 in this simulation [18].

G. Lower and Upper Chamber Pressures

Pressure derivatives relate to the lower and upper chamber volumes, and the fluid flow rates between these chambers:

$$\begin{cases} \dot{p}_l = \beta \dfrac{A_{m1} \dot{x}_m - Q_1 + Q_3}{V_{l0} - A_{m1} x_m} \\ \dot{p}_u = \beta \dfrac{-A_s \dot{x}_s + Q_1 - Q_3}{V_{u0} + A_s x_s} \end{cases}$$

where β denotes the bulk modulus of the damping fluid, and has a value of about 1.52×10^9 N/m^2 for petroleum fluids [17]; Q_1, Q_3 are the flow rate from lower to upper chamber, and that from upper to lower chamber, respectively:

$$\begin{cases} Q_1 = C_{d1} A_1 \sqrt{\dfrac{2(p_l - p_u)}{\rho}} \\ Q_3 = C_{d1} A_3 \sqrt{\dfrac{2(p_u - p_l)}{\rho}} \end{cases}$$

where C_{d1} is the discharge coefficient of 0.7 in this study, which is sufficient for design purpose [16].

H. Top Chamber (Air Reservoir)

Pressure change rate in the top chamber can be defined as:

$$\dot{p}_t = \gamma \frac{p_t A_s \dot{x}_s}{V_{t0} - A_s x_s}$$

I. The Entire System

The entire model can be expressed using the previous derivations. These formulae represent a 15th order dynamic system. We are interested in the system outputs, position and velocity of the main piston.

IV. SIMULATION AND DISCUSSION

A. Conditions

The dimensions and masses involved in this simulation are evaluated from the CAD system. The complete parameter list is collected in TABLE . The Runge-Kutta method is employed to solve these ODEs [19]. Sampling time during the simulation is 3.7037e-4s, attentively tracking the dynamics with 720 data points per round in the 225rpm cycles. Deformation of structures and frictional forces between the pistons and cylinders are not considered in this model.

B. Results

The simulation result is shown in Fig. 9. Various quantities are normalized and combined in the same plot for the convenience of comparison.

Refer to subplot (a), "F_m" indicates the sinusoidal driving force to impel the main piston, having the maximum value

788.22N. The main piston starts to oscillate with the input force after a 0.05s delay, caused by the throttling effect of the spool valves. The maximum value of the main piston displacement is 66.41e-3 m. The separation film coincides with main piston's normalized oscillation approximately with a displacement of 43.32e-3 m.

TABLE I
PARAMETERS AND VALUE EMPLOYED IN THIS STUDY

Category	Object	Nomen.	Value
Mass of…(kg)	main piston	m_m	0.2363
	separation film	m_s	1.0000e-3
	contraction spool valve	m_{cn}	1.2200e-4
	rebound spool valve	m_{rn}	
	contraction QR valve	m_{cb}	2.5460e-4
	rebound QR valve	m_{rb}	
Sectional area of… (m^2)	upside main piston	A_{m1}	3.8708e-4
	downside main piston	A_{m2}	3.3681e-4
	main piston rod	A_{m3}	5.0265e-5
	contraction spool valve (effective)	A_{cn}	1.0179e-5
	rebound spool valve (effective)	A_{rn}	
	separation film	A_s	5.9188e-4
	contraction QR valve (effective)	A_{cb}	7.9173e-6
	rebound QR valve (effective)	A_{rb}	
Initial volume of…(m^3)	bottom chamber	V_{b0}	3.3681e-5
	lower chamber	V_{l0}	3.8708e-5
	upper chamber	V_{u0}	3.1962e-5
	top chamber	V_{t0}	
Initial pressure in…(Pa)	bottom chamber	P_{b0}	1.0134e5
	lower chamber	P_{l0}	
	upper chamber	P_{u0}	
	top chamber	P_{t0}	
Spring constant of…(N/m)	contraction spool valve	k_{cn}	0.9555
	rebound spool valve	k_{rn}	
	contraction QR valve	k_{cb}	1.4333
	rebound QR valve	k_{rb}	
Bulk modulus (N/m^2)		β	1.4911e9
Specific heat ratio		γ	1.4
Rotational speed of driving force (rad/s)		w	23.5619
Driving force amplitude (N)		F_0	784.8
Discharge coefficient of spool valves		C_{d1}	0.7

The force(F_m) to main piston displacement(D)/velocity(V) plot is given in subplot (b). The F_m-D curve can be ignored since the proposed mechanical design is a velocity-sensitive fluid structure and irrelevant to the piston displacement. The maximal absolute value of force occurs when displacement is zero, since the piston reaches its maximal velocity when it passes the neutral position. The top-right corner of the F_m-V curve represents this phenonemon, saying the maximum velocity is 0.85m/s. The damper shows a rigid-style fork when the normalized velocity is about 0.1, while it shifts to a soft-style suspension when velocity is about 0.2-0.5. This curve is more preferable for riders because it reveals a lower speed damping for a good yet firm controlled feeling, and less high-speed damping for a more comfortable ride on square-edged bumps.

Subplot (c) is generated from piston velocity with respect to $F_m / \dot{x}_m$, which represents the equivalent damping coefficient.

Data points nearby zero velocity imply the mathematical transient state of the dynamic system, feasible to be disregarded in this study. However, the remaining portion of the curve shows a downside tendency approaching to zero coefficients as the piston velocity increases, achieving a different style against the constant value of a traditional damper.

V. CONCLUSION

This research proposed an innovative fluid damper design utilized in a suspension fork and modeled the high-order system dynamics. The simulation result explains that the proposed damper appears to be firmer when it run into a smooth road surface, the bicycle rider is pedaling hard or the automobile driver is steering, because the input force or velocity of the force is relative small. On the other hand, the damper becomes softer when the rider enters to a terrain route. More important, the switching processes are automatically achieved without any manual or electric operation.
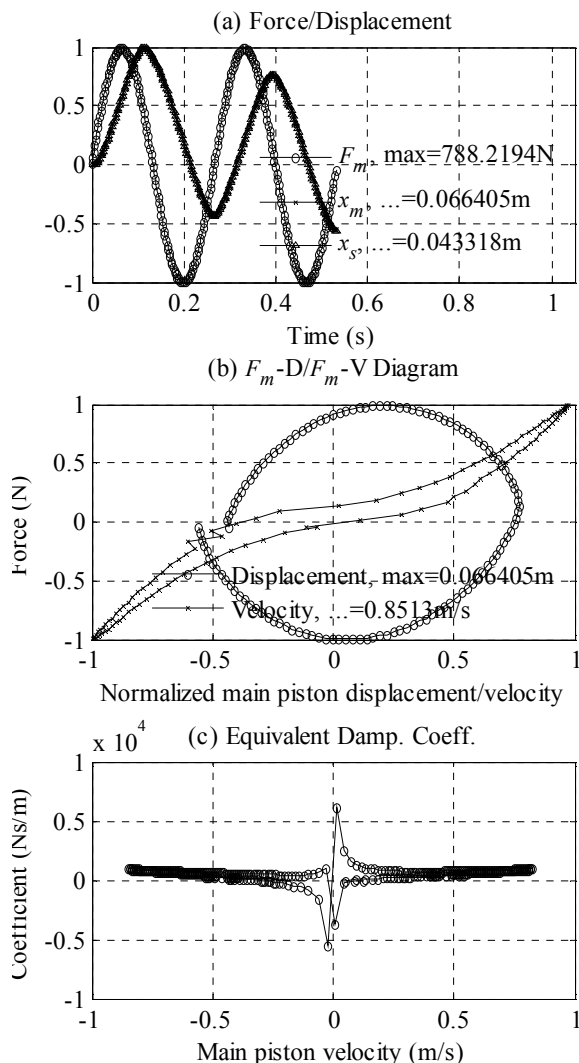
The proposed design can reduce the cost by eliminating the lockout-related components. Furthermore, it can improve the rider convenience and safety since the frequently operations are omitted. This design consumes no electric power to operate, feasible to be equipped on low-powered or powerless vehicles such as bicycles.

Further works cover (1) composing a more comprehensive system model for the cavitation occurring during heavy load and rapid piston movements; (2) forming a computational fluidic dynamic analysis model to virtually confirm the proposed theoretical model; and (3) constructing a damper prototype and a dynamic test rig to experimentally verify the mathematical model.

Fig. 9 Simulation results of the damper system

REFERENCES

[1] J. Y. Wong, Theory of ground vehicles, 2nd Ed., John Wiley & Sons Inc., 2001.
[2] T. D. Gillespie, Fundamentals of vehicle dynamics Society of Automotive Engineers Inc., 1992.
[3] "The Bose Suspension System – resolving the conflict between comfort and control," Bose Learning Center, 2008. Available: http://www.bose.com/controller?event=VIEW_STATIC_PAGE_EVEN T&url=/learning/project_sound/suspension_components.jsp
[4] Y. Shen, M. F. Golnaraghi and G. R. Heppler, "Load-leveling suspension system with a magnetorheological damper," Vehicle System Dynamics, Vol. 45 No. 4, 2007, pp. 297-312.
[5] A. Mehdi, "Semiactive fuzzy logic control for heavy truck primary suspensions: Is it effective?" SAE Transactions, Vol. 114 No. 2, 2005, pp. 157-165.
[6] R. Mollica and K. Youcef-Toumi, "A nonlinear dynamic model of a monotube shock absorber," Proceedings of American Control Conference, Albuquerque, NM, USA, 1997, pp. 704-708.
[7] F. D. Goncalves, Dynamic analysis of semi-active control techniques for vehicle applications, Master of Science in Mechanical Engineering, Virginia Polytechnic Institute and State University, 2001.
[8] K. J. Bathe, H. Zhang and S. Ji, "Finite element analysis of fluid flows fully coupled with structural interactions," Computers and Structures, Vol. 72, 1999, pp. 1-16.
[9] A. Beghi, M. Liberati, S. Mezzalira and S. Peron, "Grey-box modeling of a motorcycle shock absorber for virtual prototyping applications," Simulation Modelling Practice and Theory, Vol. 15 No. 8, 2007, pp. 894-907.
[10] P. Yang, Y. H. Tan, J. M. Yang and N. Sun, "Measurement, simulation on dynamic characteristics of a wire gauze-fluid damping shock absorber," Mechanical Systems and Signal Processing, Vol. 20 No. 3, 2006, pp. 745-756.
[11] E. L. Wang and M. L. Hull, "A model for determining rider induced energy losses in bicycle suspension systems," Vehicle System Dynamics, Vol. 25 No. 3, 1996, pp. 223-246.
[12] V. Pracny, M. Meywerk and A. Lion, "Full vehicle simulation using thermomechanically coupled hybrid neural network shock absorber model," Vehicle System Dynamics, Vol. 46 No. 3, 2008, pp. 229-238.
[13] C. Heritier, Design of shock absorber test rig for UNSW@ADFA Formula SAE car, Initial Thesis Report, School of Aerospace Civil and Mechanical Engineering, Australian Defense Force Academy University of New South Wales, 2008.
[14] J. Titlestad, T. Fairlie-Clarke, M. Davie, A. Whittaker and S. Grant, "Experimental evaluation of mountain bike suspension systems," ACTA Polytechnica, Vol. 43 No. 5, 2003.
[15] D. H. Wang and W. H. Liao, "Semi-active suspension systems for railway vehicles based on magnetorheological fluid dampers,"

Proceedings of the ASME 2007 International Design Engineering Technical Conferences and Computers and Information in Engineering Conference, DETC2007-34776, 2007.

[16] H. E. Merritt, Hydraulic control systems, New York: John Wiley & Sons Inc., 1967.

[17] R. H. Warring, Hydraulic handbook, Surrey, England: Trade and Technical Press Ltd., 1983.

[18] E. C. Yeh, S. H. Lu, T. W. Yang and S. S. Hwang, "Dynamic analysis of a double tube shock absorber for robust design," JSME International Journal Series C., Vol. 40 No. 2, 1997, pp. 335-345.

[19] G. Lindfield and J. Penny, Numerical methods using MATLAB, Prentice Hall International, 2001.